

A Crack Growth Modelling in Materials with heterogeneous microstructure

Vladislav Kozák^{1,a} and Ivo Dlouhý^{2,b}

¹Institute of Physics of Material AS of the Czech Republic, Žitkova 22, 616 62 Brno, Czech Republic

²Institute of Physics of Material AS of the Czech Republic, Žitkova 22, 616 62 Brno, Czech Republic

^akozak@ipm.cz, ^bidlouhy@ipm.cz

Keywords: cohesive zone model, traction-separation law, R curve, FEM.

Abstract. The paper studies the prediction of the crack growth of the brittle and ductile fracture of the structural materials. Crack extension is simulated by means of element extinction algorithms. The principal effort is concentrated on the application of the cohesive zone model with the exponential traction separation law and on the cohesive zone modelling. Determination of micro-mechanical parameters is based on the combination of static tests, microscopic observation and numerical calibration procedures. The attention is paid on the influence of initial value of J -integral and the slope of R curve ($J-\Delta a$) which is modelled by 3D FEM. The aim of this paper can be seen in verification of the application of the cohesive model based on the exponential traction separation law, experimental and calibration procedure inevitable for the determination of the cohesive parameters for the modelling of the fracture behaviour of the intermetallic alloy TiAl. The materials used in this investigation had the composition Ti-48Al-2Cr-2Nb-1B (in at %) and Ti-46Al-0,7Cr-0,1Si-7Nb-0,2Ni and were denoted as a alloy I and alloy F at IPM.

Introduction

Cohesive crack models are nowadays widely used to analyze cracking processes in the materials. The importance of the cohesive zone approach is emphasized to analyze the localization and failure in engineering materials. The micromechanical modeling encounters a new problem that is different from assumption of continuum mechanics. The material is not uniform on the microscale but a material element has its own complex microstructure. The concept of a representative volume element (RVE) has been introduced a few years ago. The material separation and damage of the structure is described by the interface element. Using this technique the behavior of the material is split into two parts: the damage of the free continuum with arbitrary material law and the cohesive interface between the continuum elements. The general advantage, compared to classical fracture mechanics, is that, in principle, the parameters of the respective models depend only on the material and not on the geometry. These concepts guarantee transferability from specimen to components over a wide range of sizes and geometries.

The cohesive model described the separation, δ , of a material due to acting traction, T , which gives the traction separation law (TSL). Two parameters are fundamental for various functions, the cohesive strength, T_0 , and critical separation, δ_0 . If δ exceeds δ_0 , the cohesive element cannot transmit stresses any more and new surface creates and the crack extends by one element length. Since the cohesive model is a phenomenological model, there is no evidence, which form is to be taken for the TSL, $T(\delta)$. Thus cohesive law has to be assumed independently of specific material as a model of the separation process. Most authors take their own formulation for the dependence of the TSL. The exponential model is used by many authors for both the ductile and the cleavage fracture. An exponential relationship between the effective traction δ provides a decohesion model.

The $(T-\delta)$ response follows an irreversible path with unloading always direct to origin. This model represents all the features of the separation process by: (1) the shape of the cohesive traction separation curve $(T-\delta)$, (2) the local material strength by the peak traction T_0 , and, the local ductility defined by the work of separation Γ_0 given by the area under $(T-\delta)$ curve, see Fig. 1.

Barenblatt [1] suggested the cohesive conception oriented to the singularity elimination ahead the crack tip in the classical linear fracture mechanics (LELM). The narrow strip of the Dugdale [2] soft zone designed for the plastic zone estimation ahead the crack tip was considered as a type model with the narrow strip of the soft zone marked the cohesive zone. This can be described mathematically by the following equation

$$\sigma = T_0 \cdot f(\delta / \delta_0), \tag{1}$$

where f is dimensionless function describing TSL. The fundamental parameter of the cohesive zone model is the density of the cohesive energy and the separation work falling on the branch of the cohesive area defined

$$\Gamma_0 = \int_0^{\infty} T(\delta) d\delta. \tag{2}$$

The physical sense of the cohesive zone is still under discussion although the cohesive zone approach is exploited for many years. The cohesive zone thickness can be zero; the results of the modelling can not give the same results as in case of the application of the classical mechanics of continuum. Characteristics of these physical cohesive zones (T_0 , δ_0 , Γ_0 and f) can be determined by the stress and strain analysis in narrow strips.

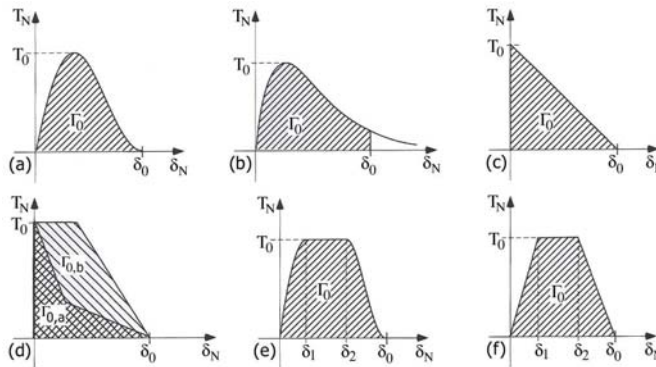


Fig. 1 Most frequently used TSLs

Cleavage fracture can be very often characterized and predicted by the LELM. The cohesive zone approach and LELM can be equivalent if the K dominant zone still exists in the closeness of the crack tip and density of the cohesive energy achieves the critical value of the dissipative energy. In this case LELM and the modelling using the cohesive zones give the same value in case if the size of the fully developed cohesive zone is given by [3]

$$\rho = \frac{4 \nu \Gamma_0}{\pi \tau_c^2}, \tag{3}$$

where Γ_0 is the cohesive energy which is equal to the energy released in case of LELM. For mode I Hilleborg [4] proposed the characteristic length of the cohesive zone

$$l_{coh} = \frac{E \Gamma_0}{(1-\nu^2) T_0^2} \quad (4)$$

It comes through that length parameter l_{coh} corresponds ρ from existing analytic calculation at the same order values. The existence of K dominance zone for coincidence achievement between cohesive zone approach and LELM is required. On condition that the cohesive zone can influence the stress distribution in distance of the crack tip given double size of the cohesive zone, the Eq. 4 can be rewrite

$$l_{coh} = \frac{K_{Ic}^2}{T_0^2} < \frac{R_k}{2}, \quad (5)$$

where R_k is the size of the K dominant zone and K_{Ic} responds $G_{IC} = \Gamma_0$. R_k is generally smaller ten times than the crack length a_0 , the inequality can be expressed in the form

$$l_{coh} = \frac{K_{Ic}^2}{T_0^2} < \frac{a_0}{20}. \quad (6)$$

Detailed discussion for elastoplastic fracture mechanics (EPLM) can be found in [3]. It was found out that the stress distribution is in the cohesive zone for slightly softened material and outside it markedly different if the maximum cohesive stress (traction) is lesser then doubles of the yield stress.

Experiments and methodic

In Table 1 one can see the chemical composition of tested materials. The alloys were produced by company Flowserve Corporation Dayton and were delivered in form of ingot about diameter of 60 mm [5].

material	Chemical composition
alloy I	Ti-48Al-2Cr-2Nb-1B
alloy F	Ti-46Al-0,7Cr-0,1Si-7Nb-0,2Ni

Table 1 Experimental material

Main goal of the experimental work was the evaluation of the flexural strength tests in the temperature range from room temperature up to 800°C (see Fig. 1). Hereafter the experiments were concentrated on the tests for fracture toughness determination utilizing the bodies with Chevron notch. For the tensile stress resistance the flat test bar about cross section 4,0 x 3,2 mm were disposed of and for the flexural strength utilizing the three and four point bending the specimens with beam structure with geometry 3,2 x 4,1 mm and length 45 mm were carry out. Fracture forces temperature dependence vs. deflection can be seen in Fig. 2. Fracture toughness experiments valuation came through specimens with the Chevron notch for the distance of rolling pin 20 mm. Fracture toughness K_{Ic} was set from the maximum force and from Chevron depth (see Fig. 3). This

procedure requires the calculation of calibration function and the critical value of the stress intensity factor can be written as

$$K_{IC} = \frac{F_{max}}{B W^{1/2}} Y_{min}^* \quad (7)$$

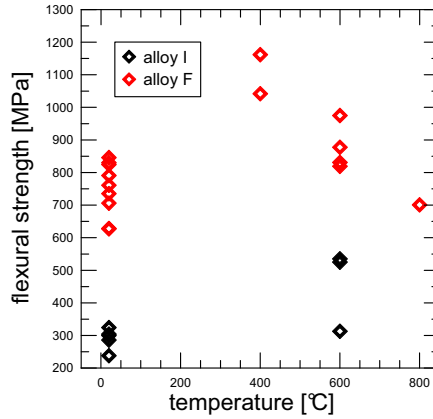


Figure 1 Temperature dependence of flexural strength for alloy I and F

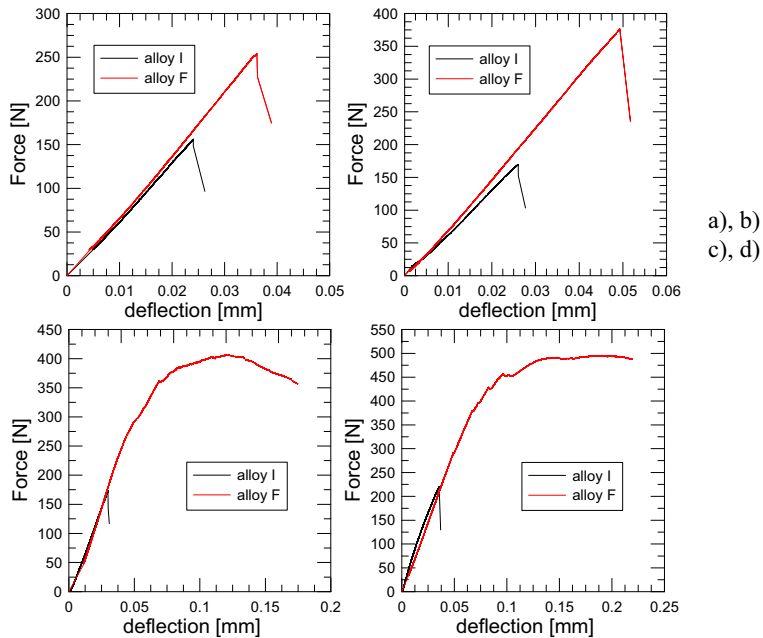


Figure 2 Temperature dependence of fracture force for temperatures:
a) 27°C, b) 400 °C, c) 600°C, d) 800°C

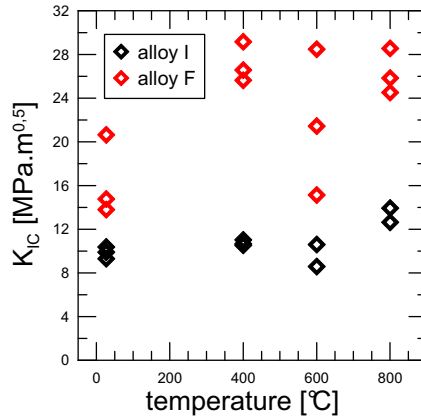


Figure 3 Fracture toughness

Numerical modeling

Linear traction separation law

The FEM mesh with two modifications was created for the stress analysis. The first one had 10000 C3D8 elements and second one 90000 elements. After some numerical test was found that there is a very small discrepancy between them and a mesh with smaller density of elements was used for next computations (see Fig. 4). The cohesive 3D elements COH3D8 with zero thickness were used for cohesive zone modeling using FEM packages Abaqus and Warp3D.

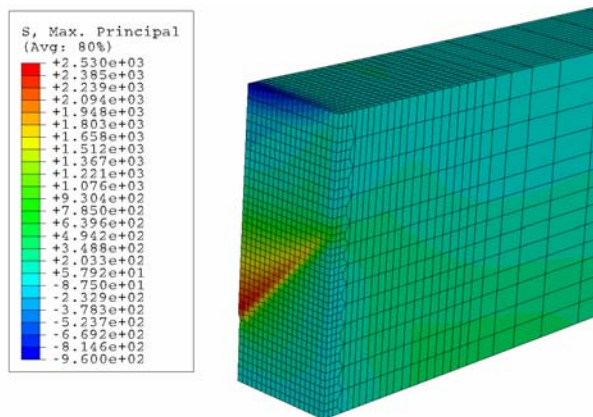


Figure 4 Maximum principal stresses before the crack growth for Chevron notch specimen

TSL embodies the linear stress arise in the damage initiation. The tested damage development can be seen in the Fig. 5 showing the linear and exponential damage development. Both models for the same material data were compared in the case of the tree point bending test with the experimental body with the Chevron notch. The input data were: Young's modulus $E=200\text{GPa}$, Poisson ratio $\nu=0,3$, the applied damage criterion was the maximum nominal deformation (MAXE),

the exponent for the exponential model was given to be 1,3. Cohesive stress $T_0 = 800$ MPa, fracture energy $\Gamma_0 = 0,5$ MPa, $\delta_c = 0,00125$ mm a $\delta_0 = 0,00023$ mm. As can be seen there is a very small discrepancy in using this two models.

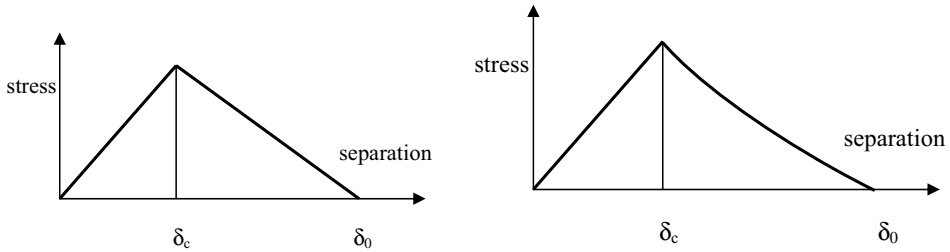


Figure 5 Cohesive models (TSL) with linear and exponential damage development

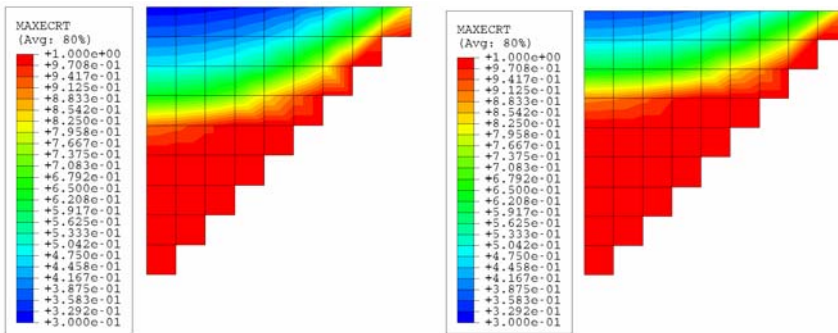


Figure 6 Maximum nominal deformation MAXE: with linear and exponential damage development ahead the crack tip

Comparing both shapes of TSL it is evident that using the exponential shape of the damage development leads to sooner damage initiation with comparing of the linear (see Fig.6).

Prediction using linear traction separation law

The input parameters of the cohesive model with linear damage development for alloy I were determined following experiments for fracture toughness. In this way the fracture energy was assigned expressing the area below the TSL. Parameter T_0 was evaluated from the values of fracture stresses. The value δ_0 was found using the area below the TSL and then by the help of δ_0 and literature [6, 7] parameter δ_c .

$$\Gamma_0 = \frac{1}{2} T_0 \delta_0 \Rightarrow \delta_0 = \frac{2 \Gamma_0}{T_0} = \frac{2,0,5}{300} = 3,33 \cdot 10^{-3} \text{ mm}, \delta_c = 3,33 \cdot 10^{-4} \text{ mm} \tag{8}$$

Procedure for the exponential traction separation law implemented in Warp3D was very similar. Obtained cohesive parameters were used in FEM computation for 3PB test. In Fig. 7 one can see differences while using both models .

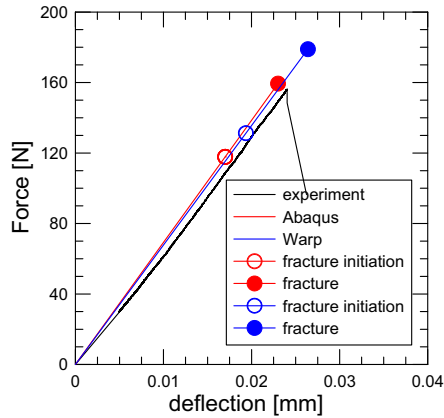


Figure 7 Crack initiation

Prediction using exponential traction separation law

The implemented cohesive elements in version of Abaqus FEM package had not supported the elastoplastic material response that is way the package Warp3D for the F alloy modelling was used. The cohesive elements with zero thickness were created using two surfaces having the same coordinates, whereas nodes of the base model are entered as a primary and then the nodes of the new created surface.

The material curve obtained for the room temperature was modified for yield stress in range from 200 to 900 MPa according [7]. Young's modulus determined experimentally was $E = 175$ GPa. J integral in Warp3D is continually computed ahead the crack tip and his positions are changing during the element killing. Thereafter the construction of the $J-\Delta a$ curve can be constructed very precisely on the assumption of Eq. 6. The crack length Δa is given by the cohesive element size, in our computations the cohesive elements have the square shape with the edge 0,08 mm (for body with Chevron notch – Fig. 8). Used values of J integral in Fig. 8 and 9 are given in moment when the entire row of elements is killed.

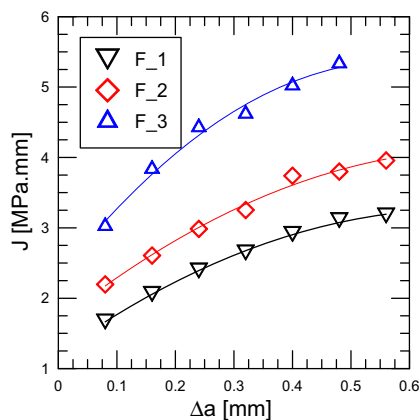


Figure 8 $J-\Delta a$ curve for $K=14 \text{ MPa}\cdot\text{m}^{0.5}$ (F_1), $K=16,36 \text{ MPa}\cdot\text{m}^{0.5}$ (F_2), $K=20 \text{ MPa}\cdot\text{m}^{0.5}$ (F_3) (body with Chevron notch, $\sigma_y=200 \text{ MPa}$)

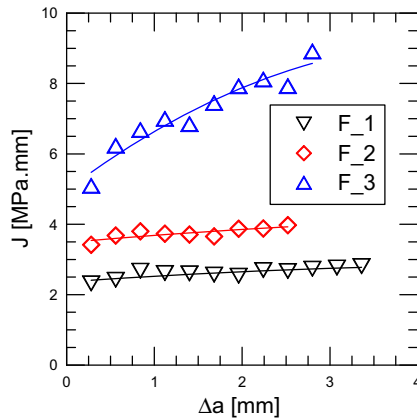


Figure 9 J - Δa curve for $K=14 \text{ MPa.m}^{0.5}$ (F_1), $K=16,36 \text{ MPa.m}^{0.5}$ (F_2), $K=20 \text{ MPa.m}^{0.5}$ (F_3), (body with sharp notch, $\sigma_y=200 \text{ MPa}$)

Summary

In conclusion, the present work has investigated the influence of local microstructure on the crack resistance for simple geometry and for material properties typical of TiAl. This work establishes the basic mechanical models, methods, and baseline results that are requisite first step toward the realistic modeling of TiAl.

These models based on the application of the cohesive zone modeling have the capacity to investigate the interplay between the local microstructure and the various material properties (mainly fracture toughness) (see [8]). Detailed analysis and possibilities of future work can be found in oral presentation.

Acknowledgement

We gratefully acknowledge the Czech Science Foundation project No: 101/05/0493 and 101/08/1304.

References

- [1] G.I. Barenblatt, *Advances in Applied Mechanics* 7 (1962), p. 55
- [2] D.S. Dugdale, *Journal of the Mechanics and Physics of Solids* 8 (1960), p. 100
- [3] Z.H. Jin, C.T. Sun, *International Journal of Solids and Structures* 43 (2006), p. 1047
- [4] A. Hillerborg, M. Modeer, P.E. Peterson, *Cement and Concrete Research* 6, (1976), p. 773
- [5] I. Dlouhý, K. Krahula, Z. Prokešová, A. Dlouhý, *Tests of Mechanical Properties and Fracture Behaviour of Ti-46Al-7Nb-0,1Cr-0,1Si-0,2Ni alloy*, report IPM AS of CZ Brno, (2006)
- [6] M. Werwer, R. Kabir, A. Cornec, A., K.-H. Schwalbe, *Engineering Fracture Mechanics* Vol. 74, Issue 16 (2007), p. 2615
- [7] R. Kabir, A. Cornec, W. Brocks, *Key Engineering Materials* Vols. 324/325 (2006), p.1317
- [8] S. Partl, *Crack Propagation Modelling in Materials with Heterogeneous Grain Microstructure*, diploma work, BUT FME and IPM AS of CZ Brno, (2007)